Monitoring the Corrosion in Columns using Fibre Optic Sensors - Preliminary Investigation

Noran Wahab [1] and Khaled Soudki [2]

[1] Post-doc at University of Waterloo, Canada (on leave from Cairo University, Egypt).
[2] Professor at University of Waterloo, Canada.

ABSTRACT: Fibre-Optic Sensors (FOSs) are being introduced for structural-health monitoring (SHM) of bridges and other structures as an attractive alternative to conventional sensors such as electrical strain gauges and vibrating wires. Advantages of the FOS, from a materials point of view, include resilience and durability. The objective of this study was to examine the feasibility of using Osmos fibre optic sensors (FOS) to record the lateral expansion due to corrosion damage in reinforced concrete (RC) columns. Four columns were tested. The columns were 200mm in diameter by 900 mm long. Each column was reinforced longitudinally with 4 15M rebars and 10M stirrups were provided at 200mm o/c. The columns were instrumented with mechanical collars and FOS sensors mounted around the circumference at mid height of the column. The longitudinal rebars in the columns were corroded to 5%, 10% and 15% mass loss using accelerated corrosion technique. During corrosion exposure, the lateral expansion due to corrosion and crack widths were monitored. The readings of the FOS and crack widths showed good correlation. The lateral expansion reached a maximum of 1.1%. Following corrosion exposure, the columns were tested axially to determine the effect of the corrosion on the column's axial capacity. The reduction in the axial capacity of the column due to corrosion was 28% with a theoretical mass loss of 15%.

Introduction

Fibre-Optic Sensors (FOSs) are being introduced to various structural engineering applications (bridges and other structures) as an alternative to conventional sensors such as electrical strain gauges and vibrating wires. Fibre-Optic Sensors (FOSs) have been used in civil engineering applications to monitor the structural behaviour on site. Some of these projects include; Esplanade Riel pedestrian bridge and Main Street Bridge in Winnipeg, Manitoba, Canada, and the Portage Creek Bridge in Victoria, British Columbia, Canada (Kim et al. (2010)).

Corrosion of steel rebars in concrete reduces their cross sectional area and produces rust that occupies a volume larger than the volume of the steel. As a result, the concrete section cracks. Reinforced concrete columns and piers are subjected to high compressive loads that are resisted by the un-cracked concrete cross section and the full cross section of the reinforcing steel rebar. Therefore, concrete cracking and the reduction in the cross section of the steel rebar caused by corrosion is detrimental to the reinforced concrete columns.

Some researchers tried measuring the lateral expansion due to corrosion and correlating it with the mass loss values (Lee et al. (2000) and El Maaddawy et al. (2006)). Most of the previous work focused on restoring the column's performance using carbon fibre wraps (Lee et al. (2000), Debaiky et al. (2006), Aquino and Hawkins (2007) and El Maaddawy (2008) and Bae and Belarbi (2009)). More experimental work is required using different concrete cover thicknesses and bar diameters to correlate the lateral expansion due to corrosion with the mass loss values. In addition, analysis was proposed to predict the capacity of the corroded un-strengthened and strengthened columns based on some experiments, but more data is required to refine the analysis (Tapan and Aboutaha (2011) and Bae and Belarbi (2009)).

The experimental work reported here is a preliminary phase of a larger experimental study that aims to investigate the feasibility of using FOS to measure the expansion due to corrosion in reinforced concrete columns. In addition, the reduced axial capacity of a corroded column is determined experimentally and verified using equations available in the literature.

Test Program

Test specimen
Four circular reinforced concrete columns were cast in the Structures Laboratory at the University of Waterloo. One column was kept as a control specimen (un-corroded). The remaining columns were corroded to different corrosion levels (5%, 10% and 15% mass loss). The columns were 200mm in diameter and 900 mm long. All the columns were reinforced longitudinally with 4 reinforcing bars as shown in Table 1. The notation is as follows; the first number stands for the column diameter; C200 is a 200mm diameter column. The following number stands for the rebar diameter. The third number represents the target corrosion level and the last number represents the concrete cover to the longitudinal reinforcing bar. In order to minimize the confinement effect, the stirrups in the transverse direction in the columns were spaced at 200 mm, which is the maximum spacing allowed in the Canadian concrete design code (CSA A23.1-04).

An anode and a cathode are required for corrosion as will be explained latter. Each corroded specimen had 2 hollow stainless steel tubes (16mm outside diameter) to act as cathodes while the reinforcing bars acted as anodes. The clear distance between the stainless tube (cathode) and the reinforcing bars (anode) was 30mm.

Table 1: Test matrix

Column	Column corrosion level (%)	Diameter (mm)	Reinforcement	Concrete cover to rebar (mm)	Theoretical corrosion time (days)
C200-M15-0%-30	0%				----
C200-M15-5%-30	5%				31
C200-M15-10%-30	10%	200	4-15M	30	62
C200-M15-15%-30	15%				94

Specimen fabrication
Sonatubes resting on double base plywood was used as the formwork to construct the columns as shown in Figure 1. Holes were pre-drilled into the base to hold the cage and the stainless steel tube in place during casting. To avoid a short circuit during the corrosion process, the steel stirrups were coated and separated from the longitudinal steel using electrical tape at the contact points (Figure 1).

Concrete was supplied by a local ready mix plant. To induce corrosion, 3.5% chlorides by weight of cement were added to the fresh concrete mixture resulting in salted concrete. Salted concrete was used to cast the middle part of a column (600 mm height). To avoid corrosion of the steel at the column ends (150mm height), these sections were cast with un-salted concrete as shown in Figure 1. Standard concrete cylinders (100 mm x 200 mm) were made from the salted and un-salted concrete mix for compressive strength testing.

The specimens were cured for 7 days by spraying them with water twice daily and covering them with wet burlap and plastic. After 7 days, the columns were stripped and stored until reaching 28 days. After 28 days, standard cylinders were tested to determine their compressive strength. Corrosion started when the columns were at least 28 days old. The salted and un-

salted concrete's strength at 28 days was 32 and 42 MPa, respectively. The salted and un-salted concrete's strength at 167 days (day of testing of the columns) was 35 and 45 MPa, respectively.
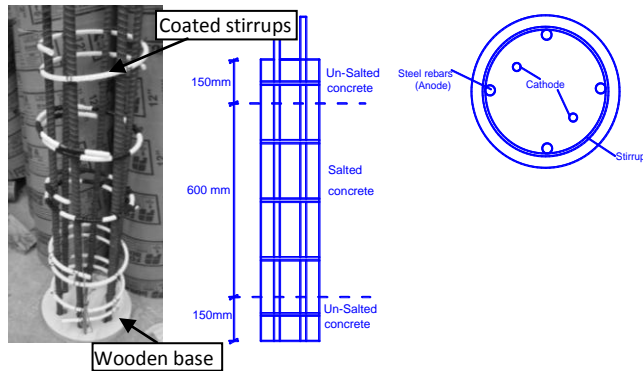

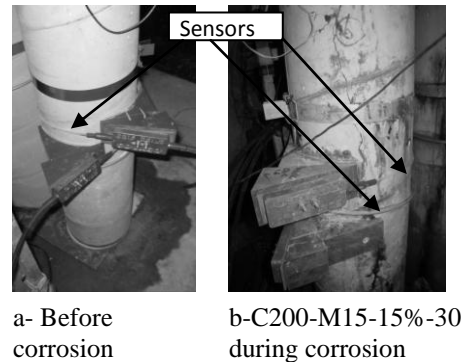Figure 1: Preparation of the specimen

a- Before corrosion

b-C200-M15-15%-30 during corrosion

Figure 2: Columns before and during corrosion

Instrumentation

Osmos FOS strands with lengths of 1m and 500mm were used to monitor the corrosion expansion in the columns. The sensor's resolution is 0.001mm. The measuring accuracy is 2% of the final value during long term monitoring. The measuring frequency is 100Hz. The response speed is infinite. The sensors are connected to the Osmos monitoring station via a customizable fibre optic cable.

In this study, one column was monitored with 1-1meter Osmos FOS strands and one column was monitored with two Osmos FOS strands (1m long strand and 500mm long strand) as shown in Figure 2. The column dimensions used in this study were small (200mm diameter) to be practical for a laboratory investigation. Hence, special PVC blocks were used to mount the sensors onto the columns and to maintain the mounting plates of the FOS sensors tangent to the column.

Mechanical collars were used in addition to the FOS sensor to measure the lateral deformation of the columns due to corrosion. The mechanical collars were mounted around the circumference of the columns and held in place using 2 springs. The right angles at the end of the collar were notched to measure the opening each time at the same location using a pointed micrometer (Figure 2).

Accelerated corrosion technique

Accelerated corrosion technique was used to induce corrosion in a reasonable amount of time. The reinforcing steel bars act as anodes while the stainless steel tubes act as cathodes. To maintain high moisture and oxygen levels, the specimens were subjected to wet and dry cycles. The salt added to the concrete mix was above the corrosion initiation threshold (ACI 222, 2001). To accelerate the corrosion process, the specimens were connected to external power supplies. Each specimen had 4 reinforcing bars (anodes) and 2 stainless steel tubes (cathodes). Therefore, each column consisted of 2 cells where a cell is composed of two reinforcing bars (anodes) connected to one stainless steel tube (cathode). The cells were connected in series. Then, the specimens were connected in series to the power supply.

The theoretical mass loss was calculated for each exposure time using Faraday's law (Table 1). The current density used was equal to 200 $\mu A/cm^2$ as recommended by El-Maaddawy and Soudki (2003) to ensure that the concrete strains and crack widths remain similar as those

experienced in the field. The length used in computing the current was the salted region length (600mm). Previous experiments indicated that at higher corrosion levels, the actual mass loss is usually less than the theoretical mass loss (estimated from Faraday's law). Therefore, all columns were corroded for a 20% extra time to ensure that reasonable corrosion levels are reached.

Mass loss analysis

The rebars in the columns were extracted a t the end of the corrosion exposure following load testing the columns to determine the actual mass loss. Mass loss analysis was conducted according to ASTM standard (ASTM G1-03 (2011). The mass loss is calculated according to Equation 1.

$$\text{mass loss}(\%) = \frac{\text{mass of un corroded rebar} - \text{mass of corroded rebar}}{\text{mass of un corroded rebar}} \times 100 \qquad (1)$$

Test Results

Cracking pattern

The observed cracking due to corrosion was as follows; Column C200-M15-5% had 4 longitudinal cracks coinciding on 4 rebars along the column face and one horizontal crack in the cross section. The cracks were very fine with widths ranging from 0.1 to 0.2 mm. Column C200-M15-10% had 3 longitudinal cracks coinciding on 3 rebars along the column face. Two cracks were 0.4 mm wide and the third crack was 0.2 mm wide. The cracks were filled with rust. Column C200-M15-15% had 4 longitudinal cracks coinciding on 4 different rebars along the column face. The width of the cracks ranged from 0.5 to 2.2 mm. Two cracks intercepted the 500mm and 1 m Osmos strands and another two cracks intercepted the 1 m Osmos strand twice.

Corrosion expansion

Figure 2 shows the columns during corrosion with the Osmos sensors and mechanical collars. The 500mm and 1m Osmos sensor represent about 78% and 140 % of the column's circumference, respectively. As such for the 1 m strand, some cracks were intercepted once by the strand and others were intercepted twice by the stand.

Figure 3 shows the corrosion expansion versus time. The expansion versus time recorded using the mechanical collar or Osmos sensor had similar shapes. The curves can be characterized by 3 phases. Phase 1, at low corrosion level, where the expansion is almost zero until cracking occurs. Phase 2 starts after phase 1 with a steep slope in the corrosion expansion versus time curve. In Phase 3, which starts at about 50 days, the slope of the corrosion expansion versus time curve is much flatter than that in phase 2. At low corrosion levels, the corrosion expansion from the mechanical collar and the 1m OMOS sensor were almost the same when the cracks were fine. At higher corrosion levels, with the appearance of multiple cracks, the corrosion expansion readings from the 500mm and 1 m Osmos sensor were much less than those from the mechanical collar. This is possibly because of the slip in the mounting system for the Osmos sensors. The corrosion expansion readings from the 500 mm Osmos sensor were similar to those from the 1m sensor although the 500mm sensor covers 80% of the column's circumference.

Figure 4 shows the lateral deformation versus the theoretical corrosion level. The variation between the deformation value of columns C300-M15-30-10 and C300-M15-30-15 at 10% mass loss was mainly due to the slippage occurring in the mounting system and the variation in the actual mass loss values between the 2 columns. Using this chart, the site engineer can estimate the actual mass loss based on the measured lateral expansion. More data is required to calibrate this relationship. Table 2 compares the corrosion expansion recorded by the Osmos FOS sensors and the mechanical collars at the end of the experiment and compares this data to

the corrosion expansion determined from the crack widths (summation of the crack widths divided by the perimeter of the column). The corrosion expansion determined from the summation of the crack widths was less than the expansion determined from the mechanical collar. However, the corrosion expansion recorded by Osmos FOS sensors showed good correlation with the expansion determined from the summation of the crack widths. The corrosion expansion determined from the summation of the crack widths provided a lower bound for the corrosion expansion for most specimens.

Table 2: Corrosion expansion for all the 200mm diameter columns at the end of the experiment

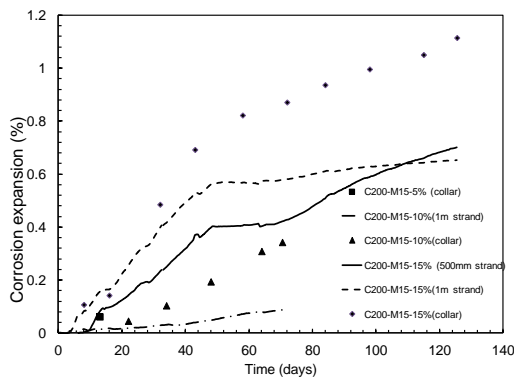| Column	Corrosion expansion (%)		
	Osmos FOS sensors	mechanical collars	Cracks widths
C300-M15-5%-30	----	----	0.127
C300-M15-10%-30	0.09 (over 1m)	0.34	0.16
C300-M15-15%-30	0.7 (over 500mm)	----	0.62 (over 500mm)
	0.65 (over 1m)	1.11	0.87 (over the perimeter)

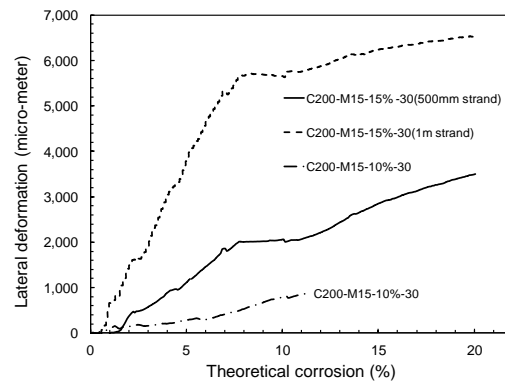Figure 3: Corrosion expansion versus time for columns 200mm diameter

Figure 4: Lateral deformation measured by Osmos sensor versus theoretical corrosion level for the 200mm diameter columns

Axial test results
The four columns were tested in axial compression following the corrosion phase. The steel rebars and the stainless tube at the ends of the columns were cut. Then, the column ends were capped with Hydrostone to provide a horizontal flat surface for loading. Although the salted concrete was provided in the middle height of the column, the longitudinal cracks extended to the full length of the column. To avoid failure at the ends during testing, each column end was wrapped with a 200mm wide Sikawrap 230 CFRP sheet. The columns were tested axially in an MTS frame in displacement controlled mode. The load was measured using a load cell and the vertical displacement was measured using the internal LVDT. In addition, the strains on the steel stirrups were measured using strain gauges.

Table 3 gives a summary of the mode of failure, peak loads and displacement for all the columns. Figure 5 shows the load versus displacement curves for all columns. The displacement increased with load until reaching the peak load. Then, the load dropped with a substantial increase in displacement. The corroded columns failed by concrete crushing and steel buckling at mid height of the column as shown in Figure 6.

The control column failed at a load of 1220 kN instead of the predicted load of 1410 kN because of a defective end capping. Columns corroded to 5% and 10% corrosion levels had almost the same peak loads of 1013 kN and 1043kN, respectively. This was 83% of the capacity of the control column. As explained in the next section, the extracted steel rebar samples from both

columns had similar percentages of mass loss. In addition, both columns showed similar cracking due to corrosion. The summation of crack widths for columns C-200-M15-5%-30 and C200-M15-10%-30 was 0.8 and 1.0mm, respectively. The column corroded to 15% mass loss (C200-M15-15%-30) had a peak load of 888 kN, or 72% of the capacity of the control column (C200-M15-0%-30). Corrosion did not seem to have any effect on the displacement of the column at peak load. The column stiffness (slope of the load versus displacement curve) decreased for the 5% and 15% corroded columns but not for the 10% corroded column in comparison to that of the control (un-corroded) column.

Figure 7 shows a typical curve for the load versus the strain of the steel stirrup. As the load increased, the strain in the stirrup increased until reaching 640με at the peak load which is well below the yield strain. Past the peak load, the confinement effect by the stirrups was more noticeable; as the load dropped from 888kN to 733kN, the strain increased from 640με to 1300 με until the test was terminated.

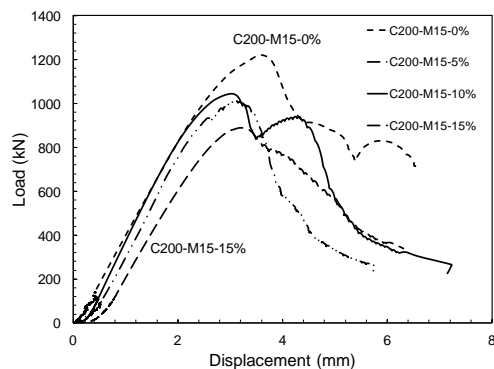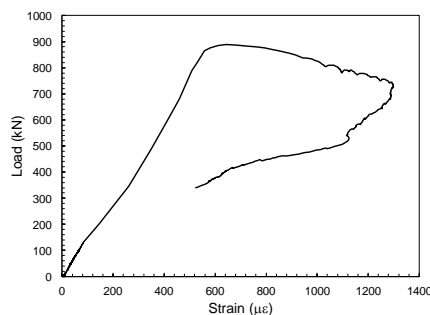Figure 5: Load versus displacement for all the 200mm diameter columns

a- Failure of control column

b-Failure of corroded columns

Figure 6: Columns after failure

Figure 7: Load versus the strain of the steel stirrup (C200-M15-15%)

Mass loss analysis

After load testing the columns, reinforcing steel bar samples were extracted from the middle section of the column using a grinder. A sample, 150 mm long, was extracted from each rebar in the column. Mass loss analysis was conducted on four extracted samples per column. It is worth noting that the analysis reflects the corrosion level at the extracted section which may or may not be the same at other sections along the rebar. The mass loss analysis results are reported in Table 4. The difference between the actual and the theoretical mass loss at lower corrosion levels is much less than the difference at higher corrosion levels. The actual mass loss per sample was much less than the theoretical mass loss particularly at higher corrosion levels. As mentioned earlier, the corrosion current used was based on a 600mm corrosion length (salted region) but the corrosion cracks occurred outside the salted region. If the same corrosion current

was used for the full height of the column, the theoretical corrosion levels for the total corrosion duration would be 4.5%, 8.5% and 12.5%.

Table 3: Test results for all the 200 mm diameter columns

Column	Mode of Failure	Peak load (kN)	Displacement at peak load (mm)
C200-M15-0%	Crushing of the capping	1220*	3.6
C200-M15-5%	Crushing of the column at mid section	1013	3.1
C200-M15-10%		1043	3
C200-M15-15%		888	3.19

* Theoretical load is 1440 kN

Table 4: Actual vs. theoretical mass loss for rebar in 200mm diameter columns

Theoretical corrosion	Actual mass loss				
	Sample 1	Sample 2	Sample 3	Sample 3	Average mass loss
5%	5.3%	4.8%	2.65%	1.2%	3.5%
10%	2.76%	1.56%	0	0	2.16%
15%	7.7%	6.4%	2.2%	2.3%	4.7%

Table 5: Experimental versus calculated loads for all the 200 mm diameter columns

Column	Experimental load (kN)	Predicted load (kN) (Based on Faraday's law)	Error (%)	Predicted load (kN) (Based on actual mass loss)	Error (%)
C200-M15-0%	1220	---	----	---	----
C200-M15-5%	1013	1045	-3.2	1051	-3.8
C200-M15-10%	1043	1025	1.7	1055	-1.2
C200-M15-15%	888	786	11.5	836	7

Calculated axial capacity

The axial capacity of corroded reinforced concrete spiral columns can be predicted using Equation 2 which was adopted from a study by Bae and Belarbi (2009).

$$P_n = 0.85 f'_c A_{eff} + f_y A_{(st)corr} \tag{2}$$

Where; f'_c is the concrete strength, f_y is the steel yield strength (in this study $f_y = 490$ MPa as reported by the manufacturer), A_{eff} is the concrete effective area, $A_{(st)corr}$ is the reduced area of the steel reinforcement, and P_n is the axial capacity of the columns. The factors 0.85 in Equation 2 accounts for the difference between the strength of the concrete loaded as a column and the strength of the concrete obtained from standard cylinder tests (ACI 318-05 (2005)). The minimum value of the concrete effective area of the corrosion-damaged column can be taken as the area enclosed by spiral reinforcement. In this study, columns with 5% and 10% theoretical corrosion levels showed similar cracking pattern, thus it was assumed that half the cover will be cracked and that the cracks will penetrate for a depth equal to the rebar diameter. For the column with 15% theoretical mass loss, it was assumed that the cover will be fully cracked and the effective area of concrete is taken as the minimum value. The reduced area of the steel reinforcement could be determined from Faraday's law or from the actual mass loss analysis. Table 5 compares the experimental versus the calculated load using Equation 2. The calculated and the measured capacity of the corroded columns were in good agreement. The main source of error can be attributed to the assumptions made in estimation of the concrete effective area. In general, the proposed equation provides a good estimate for the capacity of the corroded RC columns.

Concluding Remarks

The main findings of this study can be summarized as follows:

1-The Osmos FOS sensors functioned well in the corrosive environment and provided continuous monitoring of corrosion damage (expansion) in corroded RC columns. The maximum expansion at the end of the corrosion exposure using the Osmos sensor measurements showed good correlation with the expansion determined from the summation of cracks around the column circumference. Proper installation and calibration of the Osmos sensors is essential to obtaining reliable data.

2-Farady's law can be used to predict low corrosion levels (5% theoretical mass loss) but appears to be very un-conservative for high corrosion levels (15% theoretical mass loss) where the average experimental mass loss was much less than the theoretical mass loss.

3-The corrosion expansion with time recorded using the Osmos FOS sensor or the mechanical collar had the same shape that was characterized by 3 phases. In phase 1, the expansion was negligible until cracking occurs. In phase 2, the expansion increased with time at a steep slope where cracks grew wider and new cracks formed. In phase 3, the slope of the expansion versus time was flat. The widths of the cracks were almost the same as in phase 2, but rust could be seen on the outside surface of the cracks.

4- The corrosion expansion by the Osmos sensor and the mechanical collar were similar at the early stages of corrosion. As corrosion progressed, the expansion by mechanical collar was higher than that measured by the Osmos sensors.

5- The maximum expansion values obtained by the sensors showed a good correlation with the expansion determined based on summation of crack widths.

6-Corrosion of the longitudinal reinforcement to an average experimental mass loss of 3.5 % and 4.7% caused a reduction in the axial load capacity of the column by 17% and 28%, respectively.

7-A model was proposed to predict the axial load capacity of the corroded columns. The calculated versus measured capacity of the corroded columns were in good agreement.

References

American Concrete Institute. 2005. *Building code requirements for structural concrete.* ACI Committee 318, Farmington Hills, Michigan, USA.

ASTM. 2011. *Standard practice for preparing, cleaning, and evaluating corrosion test specimens.* ASTM G 1-03, West Conshohocken, Pa, USA.

Aquino, W. and Hawkins, N.M. 2007. Seismic retrofitting of corroded reinforced concrete columns using carbon composites. *ACI Structural Journal.*104:348-356.

Bae, S.W. and Belarbi, A. 2009. Effects of corrosion of steel reinforcement on RC Columns wrapped with FRP Sheets. *Journal of Performance of Constructed Facilities.* 23:20-31.

CSA A23.3.2004. Design of concrete structures. Canadian Standards Association, Ontario, Canada.

Debaiky, A.S., Green, M.F. and Hope, B.B. 2006. Long-term monitoring of carbon fiber-reinforced polymer wrapped reinforced concrete columns under severe environment. *ACI Journal.* 103:226-234.

El Maaddawy, T. and Soudki, K. 2003. Effectiveness of impressed current technique to simulate corrosion of steel reinforcement in concrete. *ASCE Material Journal.*15: 41-47.

El Maaddawy, T., Chahrour, A. and Soudki, K. 2006. Effect of fiber-reinforced polymer wraps on corrosion activity and concrete cracking in chloride-contaminated concrete cylinders. *Journal of Composites for Construction.* 10:139-147.

El Maaddawy, T. 2008. Behavior of corrosion-damaged RC columns wrapped with FRP under combined flexural and axial loading. *Cement and Concrete Composites.* 30:524-534.

Kim, Y.J., Murison, E. and Mufti, A. 2010. Structural health monitoring: a Canadian perspective. *Proceedings of the Institution of Civil Engineers.* 163:185-191.

Lee, C., Bonacci, J.F., Thomas, M.D.A., Maalej, M., Khajehpour, S., Hearn, S., Pantazopoulou, S. and Sheikh S. 2000. Accelerated corrosion and repair of reinforced concrete columns using carbon fibre reinforced polymer sheets. *Canadian Journal of Civil Engineering.* 27:941-948.

Tapan, M. and Aboutaha, R.S. 2011. Effect of steel corrosion and loss of concrete cover on strength of deteriorated RC columns. *Journal of Construction and Building Materials.*25: 2596–2603.